Magnetic fluctuations in nanosized goethite (α-FeOOH) grains

2009 J. Phys.: Condens. Matter 21 016007

(http://iopscience.iop.org/0953-8984/21/1/016007)

J. Phys.: Condens. Matter **21** (2009) 016007 (11pp) doi:10.1088/0953-8984/21/1/016007

Magnetic fluctuations in nanosized goethite (α-FeOOH) grains

D E Madsen[1], L Cervera-Gontard[2], T Kasama[3], R E Dunin-Borkowski[2], C B Koch[4], M F Hansen[5,6], C Frandsen[1] and S Mørup[1]

[1] Department of Physics, Building 307, Technical University of Denmark, DK-2800 Kongens Lyngby, Denmark
[2] Center for Electron Nanoscopy, Building 307, Technical University of Denmark, DK-2800 Kongens Lyngby, Denmark
[3] Department of Materials Science and Metallurgy, University of Cambridge, Pembroke Street, Cambridge CB2 3QZ, UK
[4] Department of Natural Sciences, Faculty of Life Sciences, University of Copenhagen, Thorvaldsensvej 40, DK-1871 Frederiksberg C, Denmark
[5] Department of Micro- and Nanotechnology, Technical University of Denmark, DTU Nanotech, Building 345 East, DK-2800 Kongens Lyngby, Denmark

E-mail: Mikkel.Hansen@nanotech.dtu.dk

Received 23 September 2008, in final form 10 November 2008
Published 8 December 2008
Online at stacks.iop.org/JPhysCM/21/016007

Abstract

Mössbauer spectra of antiferromagnetic goethite (α-FeOOH) particles usually show an asymmetric line broadening, which increases with increasing temperature, although the magnetic anisotropy is expected to be so large that magnetic relaxation effects should be negligible. By use of high resolution transmission electron microscopy we have studied a sample of goethite particles and have found that the particles contain many defects such as low angle grain boundaries, in accordance with previous studies of other samples of goethite particles. Such defects can result in a magnetic mismatch at the grain boundaries between nanometer-sized grains, leading to a weakened magnetic coupling between the grains. We show that the Mössbauer data of goethite can be explained by fluctuations of the sublattice magnetization directions in such weakly coupled grains. It is likely that the influence of defects such as low angle grain boundaries also plays a role with regards to the magnetic properties in other antiferromagnetic nanograin systems. We discuss the results in relation to Mössbauer studies of α-Fe_2O_3 and α-Fe_2O_3/NiO nanoparticles.

(Some figures in this article are in colour only in the electronic version)

1. Introduction

Crystallographic defects can have a significant influence on the magnetic properties of materials. In ferromagnetic materials, domain walls may be trapped by, for example, dislocations and grain boundaries, and therefore structural defects usually increase the coercivity. However, in nanocrystalline ferromagnets small grain sizes can lead to ultrasoft magnetic properties in accordance with the random anisotropy model [1, 2]. In ferrimagnets, defects such as vacancies, substituted diamagnetic ions and missing neighbor atoms at surfaces can lead to localized spin-canting, which may result in a reduced magnetization [3–5]. The influence of defects in antiferromagnetic materials like goethite (α-FeOOH) seems, however, to be less well understood.

Goethite is a common antiferromagnetic mineral in soils and sediments on Earth [6], and it has recently also been found on Mars [7]. Goethite has an orthorhombic unit cell (space group *Pnma*), and a Néel temperature around 400 K [8, 9]. Usually, goethite appears as rod-shaped nanoparticles, both when formed in Nature and when synthesized in the laboratory. The sublattice magnetization directions are close to the [010]

[6] Author to whom any correspondence should be addressed.

direction along which the particles are elongated [10]. In addition to cation substitution [6], natural goethite crystals often exhibit dislocations [11]. Mössbauer spectra of goethite particles commonly show an asymmetric line broadening that increases with increasing temperature, and the average hyperfine field decreases much faster with temperature than in well-crystallized goethite [9, 12–15]. Usually, Mössbauer spectra of goethite particles do not show the presence of both a doublet and a sextet with a temperature-dependent area ratio over a broad temperature range, as one would expect for superparamagnetic, non-interacting nanoparticles. Instead, the evolution of the spectra with temperature is typical for nanoparticles in which the sublattice magnetization directions fluctuate because of their small size, but the superparamagnetic relaxation is suppressed by inter-particle interactions [9, 16–21]. As the magnetic anisotropy constant of goethite is relatively large [10, 12, 22, 23], one would not expect relaxation effects for particles that are larger than about 10 nm. However, substantial line broadening has been seen even for particles that are larger than 100 nm [12, 13]. The unusual magnetic properties of goethite have led to much debate in the literature [9–16, 23, 24].

In this paper, we present studies of goethite particles by Mössbauer spectroscopy and high resolution transmission electron microscopy (HRTEM). We show that defects, such as low angle grain boundaries between small grains within larger, rod-shaped particles, may result in a substantial weakening of exchange coupling, such that the sublattice magnetization directions of the grains can fluctuate. We also discuss some puzzling observations obtained from samples of interacting nanoparticles of α-Fe_2O_3 [25] and of interacting α-Fe_2O_3 and NiO nanoparticles [17], which can be explained by a related weakening of the interface exchange interaction.

2. Experimental details

Goethite particles were prepared by the acid hydrolysis of an iron nitrate solution. 1.4 mol $Fe(NO_3)_3$ was dissolved in 700 ml 2 M HNO_3 and mixed with 2.8 l 1 M NaOH. The mixture was aged at 285 K for approximately 3900 days with periodic stirring. The precipitate was washed three times in dilute HNO_3; this was followed by extensive washing in water, and the sample was dried in air at room temperature. Below, this sample is referred to as the as-prepared sample. In an attempt to physically separate the particles and diminish their size, we also applied low energy ball-milling to the as-prepared sample (1 g) together with nanosized NaCl (5 g) as a dispersion medium [26] for 48 h, after which the NaCl was washed out. The ball-milling was performed in a Retsch planetary ball mill with an agate vial and balls and a rotation speed of approximately 200 rpm. As a bulk reference, we used a natural, well-crystallized sample from Cornwall, UK [9].

HRTEM, high angle annular dark-field (HAADF) and dark-field (DF) imaging were carried out at 200 kV using JEM-2200FS and FEI Tecnai F20 field emission gun (FEG) TEMs. Lattice images were analyzed using geometrical phase analysis (GPA), a technique that allows the quantitative measurement and mapping of displacement and strain fields by masking and inverse Fourier transforming individual Bragg spots in Fourier transforms of HRTEM images. The phase of each resulting complex image can be related to the displacement field distorting the fringes with respect to a reference lattice with high precision (up to 0.03 Å [27]).

Table 1. Sizes of goethite particles in nanometers, obtained from Rietveld refinement of XRD data and from TEM images.

Sample	d[100]	d[010]	d[001]
As-prepared			
XRD	12	20	7
TEM	3–5	40–70	5–20
Ball-milled			
XRD	7	9	5
TEM	∼9	∼9	∼9

Powder x-ray diffraction (XRD) data were obtained at ambient conditions with a Philips PW 1820 diffractometer using Cu Kα radiation. XRD data acquired from the as-prepared and the ball-milled samples showed the presence of goethite only. A Rietveld refinement of the data using FullProf software [29] was used to determine the average crystallite sizes, which are given in table 1.

^{57}Fe Mössbauer spectra were obtained with conventional Mössbauer spectrometers in the constant acceleration mode. The sources were ^{57}Co in Rh and a foil of α-Fe was used for calibration of the spectrometer at room temperature. Spectra obtained at temperatures between 80 K and room temperature were recorded in a liquid nitrogen cryostat. Spectra obtained between 20 and 80 K were recorded in a closed cycle helium refrigerator. A spectrum obtained in an applied field of 6 T was recorded in a liquid helium cryostat with a superconducting coil.

3. Results

3.1. Morphology and crystallography of goethite particles

Figure 1(a) shows a representative HRTEM image of the as-prepared sample. Figure 1(b) shows an image of the same agglomerate acquired using the HAADF detector of the microscope in scanning TEM (STEM) mode. In figure 1(b), the intensity is approximately proportional to the density and the thickness of the sample, and provides evidence that the crystals are far from perfect and contain many voids. The images show rods that are stacked with parallel [010] orientations. The dimensions of the rods, as estimated from HRTEM images, are given in table 1. The graph in figure 1(c), which was obtained using GPA, shows the change in orientation of the lattice planes between points 1 and 2 in the particle shown in figure 1(a). It shows that the (010) planes have variations in their orientation of 1°–2°. The data in figure 1(d) were obtained using HAADF tomography [28], a technique that allows the three-dimensional shapes and distributions of materials to be measured with nanometer spatial resolution. Figure 1(d) shows the three-dimensional shape and internal structure of a stack of goethite crystals, which are representative of the sample studied here.

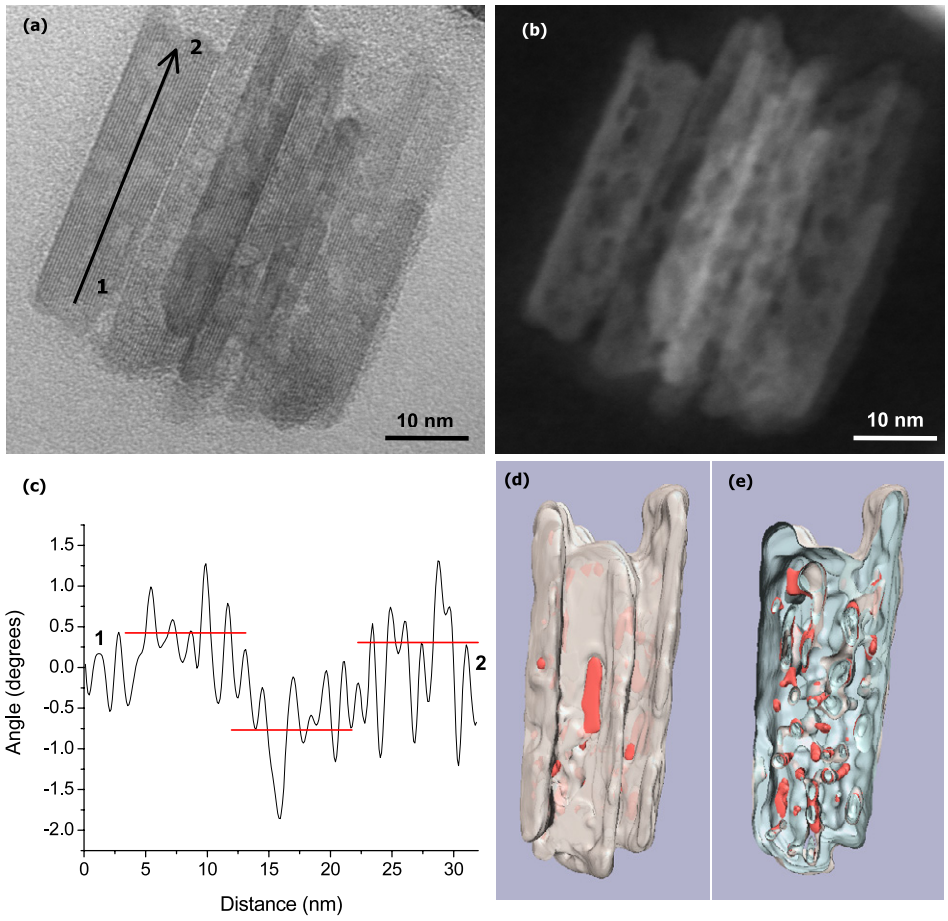

Figure 1. (a) HRTEM image of the as-prepared sample acquired in a Tecnai F20 TEM operated at 200 kV. (b) The same area imaged in the HAADF STEM mode, showing evidence of the presence of voids. (c) Changes in the orientation of the prominent lattice planes shown in (a) measured using GPA (see the text for details). The profile goes from point 1 to point 2 along the line drawn in (a). Although the graph is noisy, it clearly indicates low frequency distortions of the crystal. (d) Three-dimensional isosurface visualization of a stack of goethite crystals obtained using HAADF STEM tomography. (e) Internal structure of the same crystals revealing the presence of an interpenetrating network of voids.

Figure 1(e) shows a cut-away visualization of the same crystals revealing the presence of internal voids, which form a network that seemingly interpenetrates between the different crystals of the stack. Figure 2 shows a similar distortion in another crystal. The main cause of the change of orientation between the lower and upper parts of the crystal seems to be a grain boundary. Interpretation of the curves shown in figures 1 and 2 requires some caution because local changes in crystal thickness may affect the local values of the geometrical phase. Also, the limited size of the mask used when Fourier filtering the image degrades the resolution of the geometrical phase image and the local values of the curves correspond to values averaged over several pixels along each profile. The curves in figures 1 and 2 were obtained by integrating several profiles measured over a width of 10 pixels, and although high frequency information is not directly interpretable, the curves can still be used to measure low frequency variations in the orientation of the crystal planes, by measuring changes between minima and maxima of the profile.

Figure 3 shows an HRTEM image of part of a goethite rod, acquired using a microscope equipped with a spherical aberration corrector. The improved interpretability and resolution of this image are noticeable at the edges of the particles. Lattice fringes parallel to the long direction of the rod (the [010] direction) are visible. Closer inspection of the image reveals the presence of dislocations, and the particle is seen to consist of several grains with more or less perfect oriented attachment. Moreover, there are indications of moiré fringes, suggesting a slight relative rotation between grains in the particle.

Figures 4(a) and (b) show DF TEM images of the as-prepared and ball-milled samples, respectively. Figure 4(a) shows significant variations in contrast within the individual rods, indicating variations in crystallographic orientation. This observation is in accordance with the presence of the low angle grain boundaries and voids shown in figures 1 and 2. Figure 4(b) shows that the ball-milled sample is dominated by agglomerates of irregularly shaped particles with an average size of approximately 9 nm.

Other recent studies of the synthesis and morphology of goethite particles have shown that they can form from precursor nanoparticles of ferrihydrite, which have diameters of a few nanometers [30–34]. The ferrihydrite particles transform to goethite and this is followed by (often imperfect)

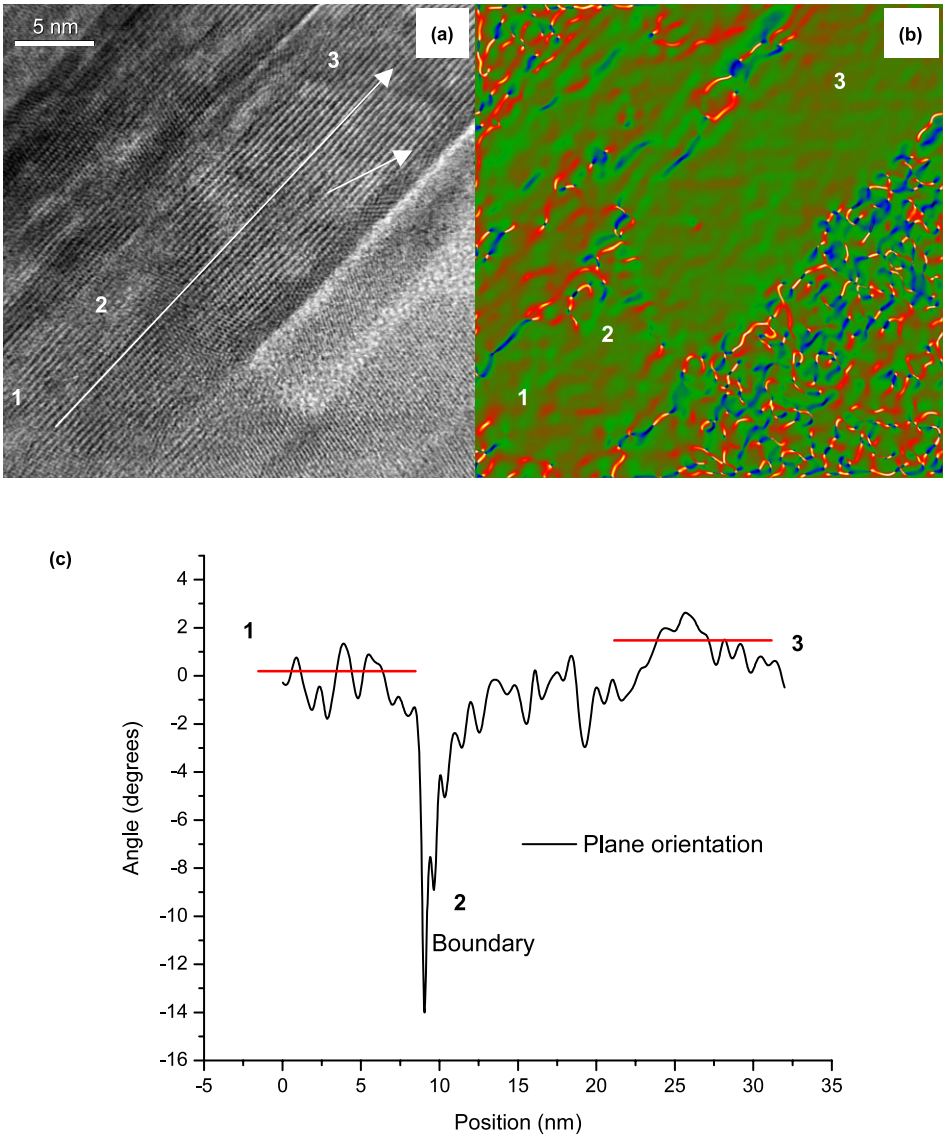

Figure 2. (a) HRTEM image of a representative crystal in the as-prepared goethite sample. (b) False-color map showing angles of the prominent lattice planes in (a) measured using GPA. (c) Line profile obtained from (b) along the line marked in (a), indicating an accumulated change of direction by approximately 2° between points 1 and 3 and a noisy signal at the grain boundary of point 2.

oriented attachment to form nanorods. Each goethite rod may be formed by the attachment of more than 100 precursor particles [34]. Inspection of HRTEM images of such rods has revealed the presence of low angle grain boundaries [30, 32, 33], with some rod-shaped goethite particles consisting of grains with dimensions of 5–8 nm [34]. Thus, defects such as low angle grain boundaries seem to be common in goethite samples prepared in different ways. Positron annihilation studies have also revealed a high concentration of defects in goethite [35], with a correlation between defect concentration and magnetic properties. Goethite particles usually contain more water and/or OH^- than predicted by the theoretical formula, and this also has an influence on the magnetic properties [15].

The dimensions of the goethite rods in the as-prepared sample, as estimated from TEM, differ considerably from the crystallite sizes estimated from XRD (table 1). The length of the rods along the [010] direction is considerably larger when measured using TEM than the [010] crystallite dimension obtained from XRD. This discrepancy suggests that the rods are not perfect single crystals, in accordance with the HRTEM observations of defects, including voids and grain boundaries, within the rods. In contrast, along the [100] direction, the dimension found using XRD is larger than that from HRTEM. This difference may be associated with oriented attachment of adjacent rods, such that the crystallographic order continues to some extent across grain boundaries [36]. Similar results were found by Bocquet *et al* [12], who compared sizes estimated from TEM and XRD for a number of synthetic and natural goethite samples. For most of the samples, the particle length estimated from TEM was considerably larger than any dimensions estimated from XRD, whereas the width of the rods, estimated from TEM, was often smaller than any of the dimensions obtained from XRD. Similar observations

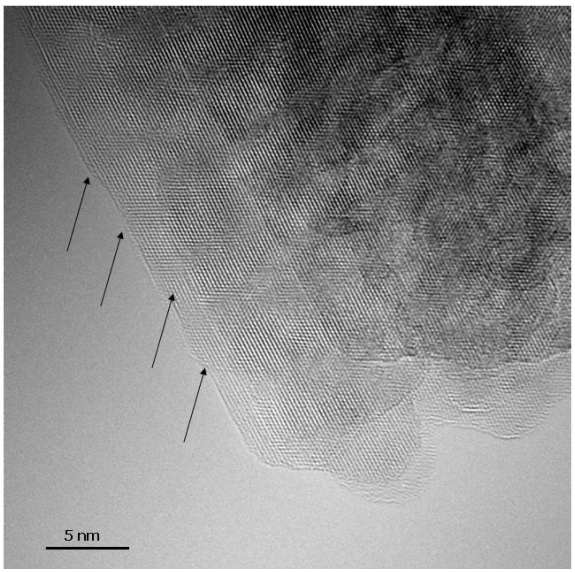

Figure 3. HRTEM image acquired in a JEM 2200 FS electron microscope operated at 200 kV with the coefficient of spherical aberration adjusted to approximately -2 μm. The image shows overlapping crystals of goethite, between which slight misorientations result in the presence of moiré fringes. The arrows show the indications of moiré fringes.

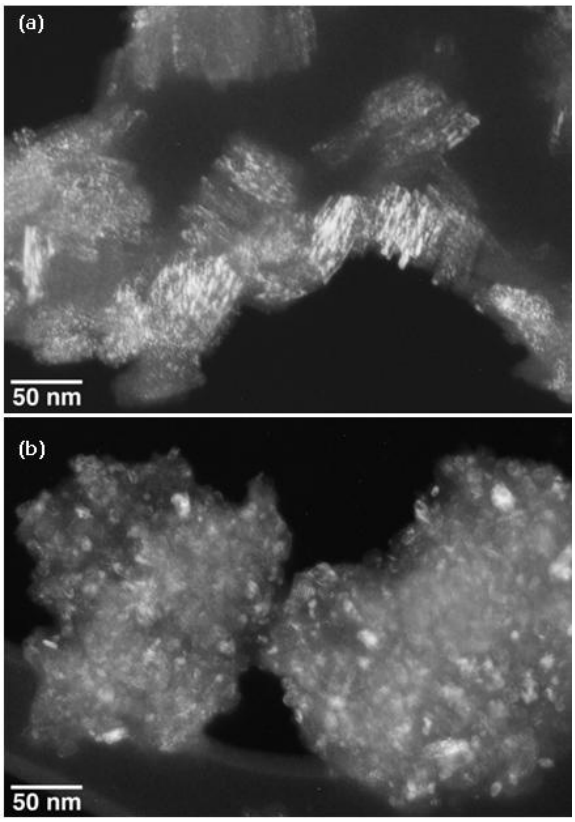

Figure 4. Single-beam DF TEM images showing crystalline domains in goethite crystals in (a) the as-prepared sample and (b) the ball-milled sample.

were also reported in a study of goethite particles with length exceeding 1000 nm [13]. Thus, the occurrence of more or less perfect oriented attachment in goethite samples appears

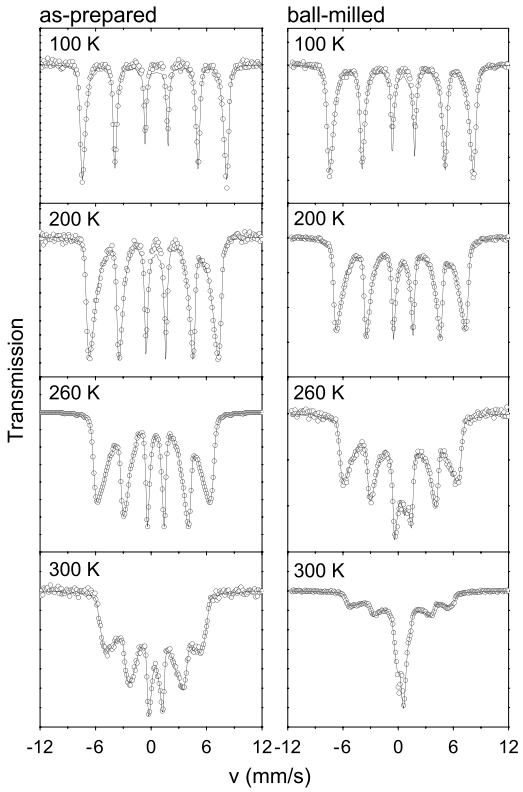

Figure 5. Mössbauer spectra of both the as-prepared and the ball-milled goethite samples obtained at the indicated temperatures. The solid line in each spectrum is a fit to a sextet with a distribution of hyperfine fields.

to make it difficult to define and measure the sizes of goethite particles in a unique way. Discrepancies between particle sizes obtained from TEM and XRD have also been found in studies of other iron oxides [6].

3.2. Mössbauer spectroscopy

Mössbauer spectra acquired from both the as-prepared and the ball-milled goethite samples are shown in figure 5. At low temperatures, the spectra consist of sextets with relatively narrow lines. At temperatures above approximately 100 K, the lines become asymmetrically broadened in a manner that is typical for goethite. Spectra acquired from the as-prepared sample show no clearly visible doublet component due to particles with fast superparamagnetic relaxation up to 300 K. In contrast, the ball-milled sample shows an intense doublet at 300 K, which is also visible at 260 K. The asymmetry of the doublet in the 300 K spectrum of the ball-milled sample can be explained by superparamagnetic relaxation times, which are not very fast compared to the timescale of Mössbauer spectroscopy, but on the order of 10^{-10} s [37]. The spectra were fitted with a distribution of sextets with different hyperfine fields, as described earlier [16, 38].

Mössbauer spectra of the as-prepared sample at 350 K in zero magnetic field and in an applied field of 6 T are shown in figure 6. The zero-field spectrum is dominated by a doublet, indicating that most of the particles are superparamagnetic or

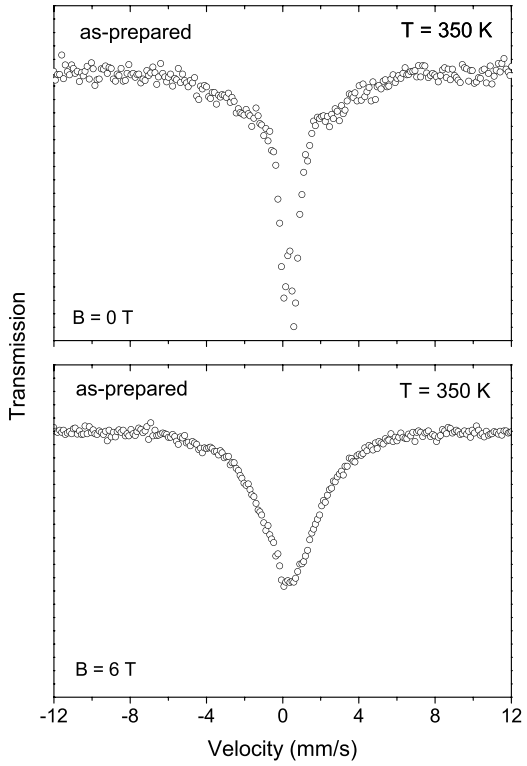

Figure 6. Mössbauer spectra of the as-prepared sample at 350 K, (a) in zero field and (b) in an applied field of 6 T.

paramagnetic at this temperature. The 6 T spectrum shows a substantial broadening of the doublet, indicating that the majority of the atoms have hyperfine fields larger than 10 T. If the sample were paramagnetic at this temperature, one would expect a broadening of the doublet component corresponding to a magnetic field at the nuclei on the order of the value of the applied field, but in superparamagnetic particles the interaction of the magnetic moments of antiferromagnetic particles with the applied magnetic field results in a significant suppression of the superparamagnetic relaxation, and this results in a substantial magnetic hyperfine splitting [16, 20]. Thus, the data in figure 6 indicate that the particles are not paramagnetic, but superparamagnetic at 350 K, in contrast to the suggestion of Bocquet *et al* [12], who interpreted the transition of goethite Mössbauer spectra from a sextet to a doublet as a Néel temperature.

4. Discussion

4.1. The superferromagnetism model

In earlier work on interacting nanoparticles, the temperature dependence of the magnetic hyperfine fields was analyzed using the 'superferromagnetism' model [9, 16, 39, 40]. In samples of antiferromagnetic nanoparticles, the dipole interaction is negligible, but there may be a strong exchange coupling between particles in close proximity [16–20]. In the model, it is assumed that the magnetic energy of a particle with volume V and magnetic anisotropy constant K, and which interacts with neighboring particles, can be written in the form

$$E = KV \sin^2\theta - \sum_{i,j} J_{ij}\vec{S}_i \cdot \vec{S}_j, \tag{1}$$

where θ is the angle between the easy magnetization direction and the sublattice magnetization vector. $\vec{S}_i$ and $\vec{S}_j$ represent the surface spins belonging to the particle and to the neighboring particles, respectively, and J_{ij} is the exchange coupling constant. K is assumed to be independent of temperature and surface effects are neglected. It should be emphasized that in general the inter-particle interaction should not be treated as an extra contribution to the uniaxial anisotropy, although this is often assumed in the literature. The interactions should rather be treated in terms of a unidirectional interaction field in accordance with the fact that low temperature hysteresis loops of field cooled samples of interacting nanoparticles show a horizontal shift (exchange bias) and not only an enhanced coercivity as one would expect if the interactions only resulted in an enhanced uniaxial anisotropy.

The influence of inter-particle interactions may be described using a mean field model, in which the summation in the last term in equation (1) is replaced by an effective interaction field acting on the sublattice magnetization of the particle [9, 16, 39, 40]:

$$E = KV \sin^2\theta - J_{\text{eff}}\vec{M}(T) \cdot \langle\vec{M}(T)\rangle. \tag{2}$$

$\vec{M}(T)$ represents the sublattice magnetization vector of the particle at temperature T and J_{eff} is an effective exchange coupling constant, such that $J_{\text{eff}}\langle\vec{M}(T)\rangle$ is the effective interaction field acting on $\vec{M}(T)$. In a study of interacting hematite nanoparticles [16], the data indicated that there was a tendency for the interaction field to be parallel to the easy direction of magnetization, in accordance with the tendency for oriented attachment of hematite nanoparticles [18]. As discussed in section 3.1, there is usually (nearly) oriented attachment of grains in samples of goethite particles. Therefore, it is reasonable to assume that the interaction field is approximately parallel to the easy direction of magnetization in the present study. Equation (2) can then be written in the form [16]

$$E(\theta) \approx KV \sin^2\theta - J_{\text{eff}}M_0^2(T)b(T)\cos\theta, \tag{3}$$

where $M_0(T)$ is the sublattice magnetization in the absence of magnetic fluctuations, which can be assumed equal to the bulk value, and

$$b(T) = \frac{|\langle\vec{M}(T)\rangle|}{M_0(T)} \tag{4}$$

is the order parameter. Assuming thermal equilibrium, the order parameter can be calculated by the use of Boltzmann statistics to take the form

$$b(T) = \frac{\int_0^\pi \exp(-E(\theta)/k_{\text{B}}T)\sin\theta\cos\theta\,\mathrm{d}\theta}{\int_0^\pi \exp(-E(\theta)/k_{\text{B}}T)\sin\theta\,\mathrm{d}\theta}. \tag{5}$$

With $E(\theta)$ given by equation (3), equation (5) can be solved numerically to find the order parameter $b(T)$, which decreases

with increasing temperature and vanishes above a critical temperature, T_p [9, 16].

The influence of magnetic fluctuations on Mössbauer spectra depends crucially on the relaxation times in relation to the timescale of Mössbauer spectroscopy, τ_M, which is on the order of a few nanoseconds. It must be realized that in general there are different types of relaxation processes in nanoparticles, namely relaxation across an energy barrier with relaxation time τ and relaxation between states in one of the energy wells. For a ferromagnetic particle exposed to a small (applied or interaction) field along the easy direction, the relaxation times for superparamagnetic relaxation, i.e., relaxation between the two energy minima at $\theta = 0$ and π, is given by [41]

$$\tau_{\pm} \cong \tau_0(1-\varepsilon^2)(1\pm\varepsilon)\exp\left[\frac{KV}{k_BT}(1\pm\varepsilon)^2\right], \qquad (6)$$

where τ_+ and τ_- are the relaxation times for relaxation processes with initial states in the lower and the upper minimum, respectively. τ_0 is in the range 10^{-13}–10^{-9} s and $\varepsilon = B_i/B_a$ where B_i is an applied magnetic field (or an interaction field) and B_a is the anisotropy field. When $\tau \ll \tau_M$, the magnetic splitting of the spectra is expected to be proportional to the average magnetization, i.e., the magnetic splitting vanishes in non-interacting particles in zero field, but if the particles are exposed to an applied field or an interaction field, a non-zero magnetic hyperfine splitting will be observed. If $\tau \gg \tau_M$, the Mössbauer spectra are magnetically split, but the magnetic splitting may be reduced compared to the bulk value, because of fluctuations of the magnetization vector close to the energy minima (collective magnetic excitations) [39, 42].

The magnetic fluctuations can be described using a multi-level model [42–44] in which a ferromagnetic particle is considered as a quantum mechanical macrospin, S^M. Thus, the particle has $2S^M + 1$ states with z-components of the spin given by S^M, $S^M - 1$, $S^M - 2$, ..., $-S^M$. The characteristic time for magnetic relaxation between states within the same energy well is on the order of τ_0 or smaller [43, 44]. Therefore, if $\tau_0 \lesssim 10^{-10}$ s it is a good approximation to assume that relaxation within an energy well is fast compared to the timescale of Mössbauer spectroscopy such that the magnetic hyperfine splitting is proportional to the average magnetization with the average taken over fluctuations within an energy well [39, 42]. If τ_0 is on the order of 10^{-10} s, the relaxation between the states within an energy well may result in a slight line broadening of the Mössbauer spectra. In antiferromagnetic nanoparticles the value of τ_0 is usually much smaller than 10^{-10} s [20] and then the relaxation between states within an energy well will be fast compared to τ_M. Although the magnetic fluctuations in antiferromagnetic nanoparticles are more complex, the relaxation can be described by a similar multi-level model [42].

For interacting nanoparticles the relative size of the two terms in equation (3) is important. If the interaction energy is predominant, there will only be one energy minimum, and the relaxation will then take place between states in this energy well and is expected to be fast, as discussed above. The magnetic hyperfine splitting can therefore be considered to be proportional to $|\langle\vec{M}(T)\rangle| = M_0(T)b(T)$. If the anisotropy energy is predominant or comparable to the interaction energy, there will be two (non-equivalent) energy minima, which are separated by an energy barrier. The transition probability per unit time for transitions across the energy barrier will be given by an expression similar to equation (6). At low temperatures, the relaxation across the energy barrier may therefore be slow compared to the timescale of Mössbauer spectroscopy, but relaxation between states within an energy well is still expected to be fast. The magnetic hyperfine splitting is then proportional to the sublattice magnetization, averaged over the fluctuations within a minimum, rather than being proportional to $|\langle\vec{M}(T)\rangle|$ [39, 42]. The magnetic hyperfine splittings will in general differ for the two non-equivalent minima. Because of the interaction field, the thermal population of the two minima will be temperature dependent. When the thermal energy is low compared to the interaction energy, the population of the upper minimum will be negligible. In this case, the observed hyperfine field will approximately be given by the thermal equilibrium value, taken over fluctuations within the lower minimum, and it will essentially be proportional to $|\langle\vec{M}(T)\rangle|$.

The distribution of anisotropy energies and interaction energies in a sample will result in a distribution of magnetic hyperfine fields at finite temperatures. Fits of the temperature dependence of the *average* hyperfine field of interacting hematite [16] and goethite [9] nanoparticles to the superferromagnetism model gave negligible values of the magnetic anisotropy energy, presumably because the influence of anisotropy is averaged out if only the average hyperfine field is fitted [16]. However, in the study of hematite nanoparticles, it was found that the temperature dependence of quantiles in the hyperfine field distribution $p(B_{hf}(T))$ gave finite values of the magnetic anisotropy energies, which were in accordance with those found for the non-interacting particles. This strongly supports the validity of the model. The quantile, f, is defined as

$$f = \int_0^{B_f(T)} p\,(B_{hf}(T))\,\mathrm{d}B_{hf}. \qquad (7)$$

In the superferromagnetism model, the values of the anisotropy energy, KV and the interaction energy parameter T_p^0 are free parameters for each quantile. T_p^0 is defined as the ordering temperature for a sample with zero anisotropy ($KV = 0$) and is given by the expression [9, 39]

$$T_p^0 = \frac{J_{eff}M(T_p^0)^2}{3k_B}. \qquad (8)$$

The interaction energy, $E_i(T) = J_{eff}M_0(T)^2b(T)$, depends on temperature because both $b(T)$ and $M_0^2(T)$ are temperature dependent. As an approximate measure of the interaction energy well below T_p we use the value $E_{int} = 3k_BT_p^0$.

4.2. The as-prepared sample

Magnetization [10] and Mössbauer spectroscopy [12, 22] studies of goethite samples with relatively large particle size and in large applied magnetic fields showed that the magnetic

anisotropy constant is relatively large, $K \approx 5 \times 10^4$ J m^{-3}, and the estimated values for three different samples were similar. In a high field Mössbauer study of a single crystal of goethite, a lower limit of $K = 6 \times 10^4$ J m^{-3} was estimated [23]. Previous studies have shown that the magnetic anisotropy constant of magnetic nanoparticles generally increases with decreasing particle size, especially for particle dimensions below 10 nm [45–47], presumably because of the influence of surface anisotropy. In the following, we assume that $K \gtrsim 5 \times 10^4$ J m^{-3} for our goethite particles.

Let us consider non-interacting particles with superparamagnetic relaxation time given by equation (6), $\varepsilon = 0$, $\tau_0 \approx 10^{-11}$ s, $K \gtrsim 5 \times 10^4$ J m^{-3} and a volume of $V \sim 1800$ nm^3, corresponding to one of the rods seen in the TEM images of the as-prepared sample. Such particles have a superparamagnetic relaxation time, $\tau \gg \tau_M$, at $T < 350$ K, and the influence of collective magnetic excitations will be almost negligible. Interactions between rod-shaped particles in close proximity may also contribute to a suppression of the relaxation. Thus, magnetic fluctuations of the spin structure of the rods as a whole cannot explain the line shapes of the Mössbauer spectra in figure 5.

The Mössbauer spectra have similarities to those of interacting hematite nanoparticles, which have been successfully analyzed by use of the superferromagnetism model [16]. In studies of hematite nanoparticles, it was possible to control the strength of the inter-particle interactions. If the particles are coated with, for example, oleic acid, the interactions are negligible, but if a suspension of uncoated particles is dried, there may be strong inter-particle interactions due to exchange interactions between surface atoms of neighboring particles [16, 17, 40]. Gentle grinding of interacting particles can significantly reduce the interaction [48], and it has been shown that the aggregation processes are reversible [19]. Similar results have been found for ^{57}Fe-doped NiO nanoparticles [21]. Mössbauer spectra of non-interacting or weakly interacting hematite nanoparticles typically consist of a superposition of a sextet and a doublet with relatively narrow lines due to particles with relaxation times that are very long or very short compared to τ_M, respectively. The relative areas of the two components depend on temperature. Due to the exponential dependence of the relaxation time on the volume, there is a very broad distribution of relaxation times, and only a small fraction of the particles have relaxation times close to τ_M. The evolution with temperature of the spectra of interacting hematite nanoparticles is quite different. Instead of the appearance of a doublet at finite temperatures, the lines of the sextet broaden, and the average hyperfine field decreases much faster with increasing temperature than the bulk hyperfine field. The distributions of magnetic anisotropy energies and of the interaction energies will result in a distribution of hyperfine fields, which leads to asymmetric line broadening in the Mössbauer spectra [9, 16–21]. The influence of interactions on the spectral shape is similar to that of an applied magnetic field [16, 40], in accordance with equation (2).

We have analyzed the temperature dependence of the magnetic hyperfine fields of the goethite sample by using the

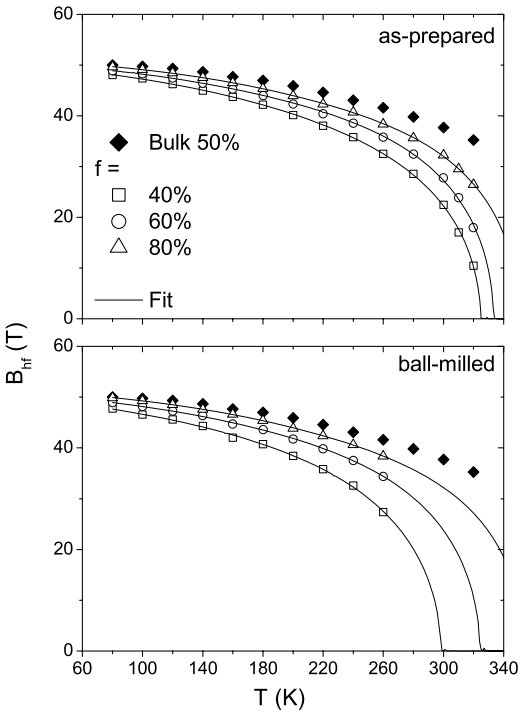

Figure 7. Temperature dependence of the magnetic hyperfine fields for the 40%, 60% and 80% quantiles for the two samples. Data for the reference (bulk) sample are shown for comparison.

superferromagnetism model. For each quantile, f, in the hyperfine field distribution, the temperature dependence of the magnetic hyperfine field $B_f(T)$, was fitted to

$$B_f(T) = B_0(T) b_f(T), \tag{9}$$

where $B_0(T)$ is the bulk hyperfine field (which is assumed to be proportional to $M_0(T)$). Data for the 40%, 60% and 80% quantiles are shown in figure 7 together with the bulk hyperfine field. The isomer and quadrupole shifts are consistent with goethite (at 20 K, we find $\delta = 0.491(1)$ mm s^{-1} and $\varepsilon = -0.117(1)$ mm s^{-1} for the as-prepared sample and $\delta = 0.492(2)$ mm s^{-1} and $\varepsilon = -0.112(2)$ mm s^{-1} for the ball-milled sample). The critical temperatures, T_p, above which the particles are superparamagnetic, are on the order of 325–350 K. Therefore, the zero-field spectrum at 350 K (figure 6) contains an intense doublet. Figure 8 shows the estimated values for the anisotropy energy KV/k_B and the interaction energy E_{int}/k_B as a function of the quantile, f. The anisotropy energy, KV/k_B varies from around 400 to 1400 K, whereas E_{int}/k_B is on the order of 800 K and varies only little as a function of the quantile. For the largest values of KV, there will be two minima of the magnetic energy. However, with $E_{int}/k_B \approx 800$ K the population of the upper minimum will be well below 1% even at 300 K and is therefore negligible. Thus, it seems to be a good approximation to assume thermal equilibrium and analyze the data using the order parameter $b_f(T)$, calculated by use of equation (5).

Using the data for the anisotropy energy KV in figure 8 and $K \gtrsim 5 \times 10^4$ J m^{-3} we find that the effective volumes of the relaxing and interacting grains are $V_g \lesssim 100$–400 nm^3

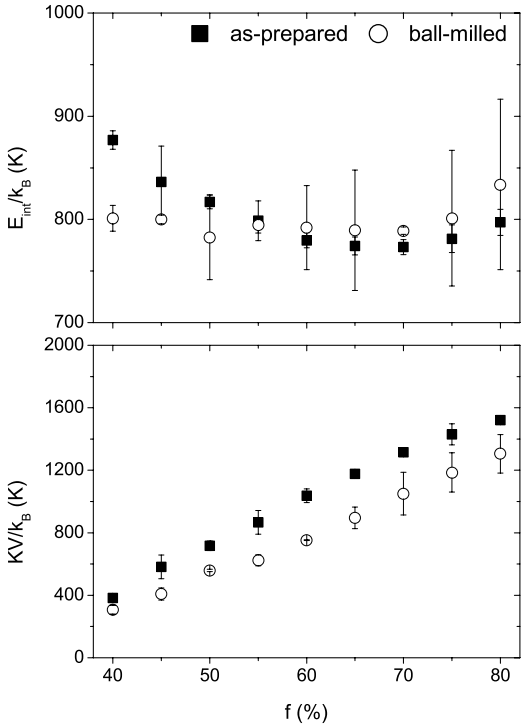

Figure 8. Values of $E_{\text{int}}/k_{\text{B}}$ and KV/k_{B} as a function of the quantile parameter f.

corresponding to grain dimensions around 5–8 nm or smaller. These volumes are much smaller than the overall sizes of the rods estimated from TEM, but similar to the typical sizes of the grains separated by defects including voids and low angle grain boundaries. This suggests that the magnetic fluctuations are governed not by relaxation of the sublattice magnetizations of the entire rod-shaped particles as a whole, but rather by magnetic fluctuations in smaller grains within them. Thus, the rod-shaped particles seem to consist of small grains with relatively weak inter-grain interactions.

It may seem surprising that defects such as low angle grain boundaries in the rod-shaped particles can result in a substantial weakening of the magnetic interaction between neighboring grains. Some low angle grain boundaries may be described in terms of dislocations. As illustrated schematically in figure 9, a simple defect such as an edge dislocation with an extra plane with a single layer of magnetic atoms, which would have negligible influence on the magnetic properties of a ferromagnet, may have a significant effect on the properties of an antiferromagnetic material. For the dislocation shown in figure 9, the sublattice magnetization direction of the extra plane cannot be antiparallel to the magnetization direction in both of the neighboring planes and will therefore cause magnetic frustration. If we neglect spin-canting, and calculate the magnetic interaction energy (the summation in equation (1)) along the dotted line in figure 9, assuming that all exchange coupling constants are equal, we find that the eight contributions to the interaction energy cancel. In practice one would expect the magnetic frustration around a dislocation to give rise to spin-canting, but in any case, such a dislocation will result in a significant weakening of the magnetic coupling.

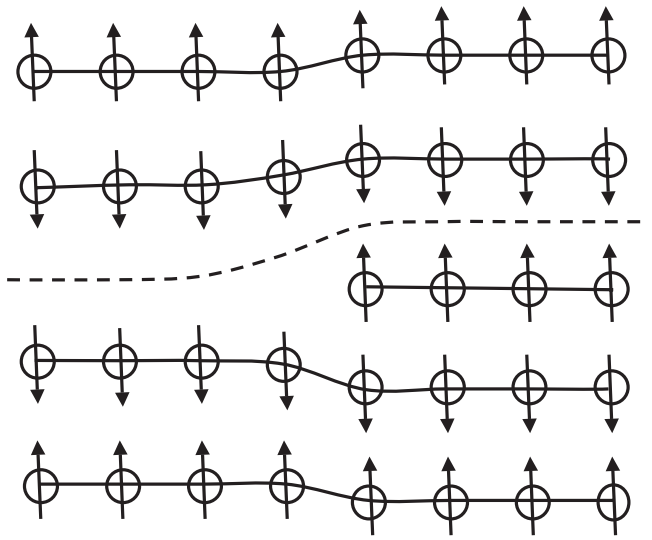

Figure 9. Schematic illustration of the magnetic structure around a dislocation in an antiferromagnetic material. Possible spin-canting is not taken into account.

A small relative rotation of grains in a particle, as suggested by the moiré fringes in figure 3, will also result in magnetic mismatch, which will weaken the coupling across the interface. Thus, although there are many atoms in close contact at an interface, the effective magnetic exchange coupling between grains (the last term in equation (1)) may be small in an antiferromagnetic material. Voids in the particles, as seen in figure 1, as well as excess water and/or OH^- [15], may also contribute to weakening of the coupling between grains. The weak coupling between grains can explain why the sublattice magnetization directions of the grains can fluctuate. Heating of goethite nanoparticles may result in stronger interactions between the grains [49, 50], indicating that some of the defects have disappeared.

4.3. The ball-milled sample

The presence of a doublet in the room temperature spectrum of the ball-milled sample indicates that fast superparamagnetic relaxation takes place in this sample. In the ball-milled sample, the particle volume, determined by both XRD and TEM, is around 300–400 nm^3 and the interaction between the particles may be small because the particles are not stacked regularly as in the as-prepared sample. We then estimate that the superparamagnetic relaxation time at 300 K for relaxation of the spin structure of a particle as a whole may be less than 1 ns if $\tau_0 \approx 10^{-11}$ s and $K \approx 5 \times 10^4$ J m^{-3}, in accordance with the presence of a doublet in the Mössbauer spectrum at 300 K.

The temperature dependence of the hyperfine fields for different quantiles and the parameters KV and E_{int}, as estimated from fits to the superferromagnetism model, are shown in figures 7 and 8, respectively, together with the data for the as-prepared sample. It is remarkable that the values of KV and E_{int} are similar for the as-prepared and ball-milled samples, although the overall particle sizes differ. This agreement supports the interpretation of the data in terms

of magnetic fluctuations in much smaller grains, which have similar sizes in the two samples.

It appears that there are two types of relaxation in the ball-milled goethite particles, namely magnetic fluctuations of the small, interacting grains within the rod-shaped particles and superparamagnetic relaxation of the spin structure of the whole particles at the highest temperatures. Below the superparamagnetic blocking temperature, such a particle will be influenced by fluctuations of the average sublattice magnetization directions of the particle as a whole (collective magnetic excitations), which result in a small reduction in the measured hyperfine field according to the expression [39, 42]

$$B_{\mathrm{f}}^{\mathrm{obs}}(T) \cong B_{\mathrm{f}}(T)\left[1 - \frac{k_{\mathrm{B}}T}{2KV_{\mathrm{part}}}\right] \tag{10}$$

where V_{part} is the volume of the whole particle. Thus the hyperfine fields of the ball-milled sample should be reduced slightly as compared to the as-prepared sample ones because of this effect. This can explain the slightly lower values of KV/k_{B} in figure 8. If we assume that $B_{\mathrm{f}}(T)$ is the same for each of the two samples and that the slightly smaller hyperfine fields in the ball-milled sample is due to collective magnetic excitations, we find that $K \approx 10^5$–10^6 J m^{-3}, i.e. somewhat larger than the values found in magnetization and high field Mössbauer studies [10, 12, 22, 23] of larger goethite particles. The difference may be due to a larger contribution from surface anisotropy in our particles.

4.4. α-Fe$_2$O$_3$ and NiO nanoparticles

On the basis of the interpretation of the goethite data, discussed above, it is relevant to discuss the Mössbauer data obtained from interacting α-Fe_2O_3 [25] and from interacting α-Fe_2O_3 and NiO nanoparticles [17]. Interaction between randomly aggregated α-Fe_2O_3 nanoparticles leads to Mössbauer spectra with a reduced absolute value of the quadrupole shift at low temperatures, indicating a rotation of the sublattice magnetization directions [25]. The effective interaction field presumably makes a finite angle with the anisotropy field of these particles, and it is likely that this leads to the observed spin rotation [25]. Interaction with NiO nanoparticles was found to result in faster superparamagnetic relaxation of the α-Fe_2O_3 nanoparticles, as compared to a similarly prepared sample with only α-Fe_2O_3 nanoparticles [17]. This observation indicates that the inter-particle interaction between α-Fe_2O_3 and NiO is weaker than the interaction between α-Fe_2O_3 nanoparticles. However, in the samples containing both α-Fe_2O_3 and NiO, a more significant spin rotation in the α-Fe_2O_3 particles was observed, suggesting a strong exchange interaction across the α-Fe_2O_3/NiO interfaces [17]. We are currently investigating the attachment of α-Fe_2O_3 and NiO nanoparticles [51]. In the case of the effective exchange field making a finite angle with the anisotropy field of the particles, the origin of spin rotation seems similar to that observed for pure α-Fe_2O_3 nanoparticle systems [25]. Additionally, if there are mismatches in the crystallographic and/or magnetic structures at the interface, then the surface spins cannot be oriented in such a way that the exchange energy is minimized for all interacting neighboring spins, leading to magnetic frustration. Such mismatches may both reduce the inter-particle interaction as in goethite and result in spin-canting, which may lead to a rotation of the sublattice magnetization directions.

5. Conclusions

By use of Mössbauer spectroscopy we have studied goethite particles that show the commonly observed asymmetric line broadening in the spectra, which has been debated in the literature for decades. We have studied goethite particles before and after ball-milling and analyzed the temperature dependence of different quantiles in the magnetic hyperfine field distribution. The data were in accordance with the superferromagnetism model, with similar anisotropy energy and interaction energy for the two samples in spite of different particle sizes. The data suggest that the temperature dependence of the spectra is due to fluctuations of the magnetization directions in grains that are much smaller than the overall particle size. The presence of such grains is supported by HRTEM studies. Magnetic mismatch at the interfaces leads to a weakened magnetic coupling between the antiferromagnetic grains such that the sublattice magnetization directions can fluctuate. Similar phenomena may occur in other antiferromagnetic nanograin systems, and we have discussed the results obtained for goethite in relation to Mössbauer studies of α-Fe_2O_3 nanoparticles and of α-Fe_2O_3/NiO nanoparticle composites.

Acknowledgments

The work was supported by the Danish Research Council for Technology and Production Sciences. Thanks are due to P A Midgley at the University of Cambridge and A I Kirkland at the University of Oxford for access to their electron microscopy facilities under the ESTEEM project (no 026019) for transnational access. We are grateful to Bente Lebech for help with the Rietveld analysis and to Mihaly Posfai for providing supporting electron microscopy observations.

References

[1] Herzer G 1995 *Scr. Metall. Mater.* **33** 1741
[2] Herzer G 1996 *J. Magn. Magn. Mater.* **157** 133
[3] Coey J M D 1971 *Phys. Rev. Lett.* **27** 1140
[4] Morrish A H and Haneda K 1983 *J. Magn. Magn. Mater.* **35** 105
[5] Mørup S 2003 *J. Magn. Magn. Mater.* **266** 110
[6] Cornell R M and Schwertmann U 2003 *The Iron Oxides: Structure, Properties, Reactions, Occurrences and Uses* 2nd edn (New York: Wiley–VCH)
[7] Morris R V *et al* 2006 *J. Geophys. Res.* **111** E02S13
[8] Forsyth J B, Hadley I G and Johnson C E 1968 *J. Phys. C (Proc. Phys. Soc) Ser. 2* **1** 179
[9] Mørup S, Madsen M B, Franck J, Villadsen J and Koch C J W 1983 *J. Magn. Magn. Mater.* **40** 163
[10] Coey J M D, Barry A, Brotto J-M, Rakoto H, Brennan S, Mussel W N, Collomb A and Fruchart D 1995 *J. Phys.: Condens. Matter* **7** 759
[11] Taitel-Goldman N, Koch C B and Singer A 2004 *Clays Clay Miner.* **52** 115

[12] Bocquet S, Pollard R J and Cashion J D 1992 *Phys. Rev.* B **46** 11657
[13] Koch C J W, Madsen M B and Mørup S 1985 *Surf. Sci.* **156** 249
[14] Murad E 1982 *Am. Mineral.* **67** 1007
[15] Barrero C A, Betancur J D, Greneche J M, Goya G F and Berqúo T S 2006 *Geophys. J. Int.* **164** 331
[16] Hansen M F, Koch C B and Mørup S 2000 *Phys. Rev.* B **62** 1124
[17] Frandsen C and Mørup S 2003 *J. Magn. Magn. Mater.* **266** 36
[18] Frandsen C, Bahl C R H, Lebech B, Lefmann K, Kuhn L T, Keller L, Andersen N H, Zimmermann M v, Johnson E, Klausen S N and Mørup S 2005 *Phys. Rev.* B **72** 214406
[19] Frandsen C and Mørup S 2006 *J. Phys.: Condens. Matter* **18** 7079
[20] Mørup S, Madsen D E, Frandsen C, Bahl C R H and Hansen M F 2007 *J. Phys.: Condens. Matter* **19** 213202
[21] Bahl C R H and Mørup S 2006 *Nanotechnology* **17** 2835
[22] Pankhurst Q A and Pollard R J 1990 *J. Phys.: Condens. Matter* **2** 7329
[23] Meagher A, Pankhurst Q A and Dickson D P E 1986 *Hyperfine Interact.* **28** 533
[24] Bocquet S 1996 *J. Phys.: Condens. Matter* **8** 111
[25] Frandsen C and Mørup S 2005 *Phys. Rev. Lett.* **94** 027202
[26] Ding J, Shi Y, Chen L F, Deng C R, Fuh S H and Li Y 2002 *J. Magn. Magn. Mater.* **247** 249
[27] Hÿtch M J, Putaux J L and Pénisson J M 2003 *Nature* **423** 270
[28] Midgley P A, Ward E P W, Hungría A B and Thomas J M 2007 *Chem. Soc. Rev.* **36** 1477
[29] CEA 1999 *LLB Powder Diffraction Software Site* http://www-llb.cea.fr/fullweb/
[30] Banfield J F, Welch S A, Zhang H, Ebert T T and Penn R L 2000 *Science* **289** 751
[31] Guyodo Y, Mostrom A, Penn R L and Banerjee S K 2003 *Geophys. Res. Lett.* **30** 1512
[32] Nesterova M, Moreau J and Banfield J F 2003 *Geochim. Cosmochim. Acta* **67** 1177
[33] Burleson D J and Penn R L 2006 *Langmuir* **22** 402
[34] Penn R L, Erbs J J and Gulliver D M 2006 *J. Cryst. Growth* **293** 1
[35] Bocquet S and Hill A J 1995 *Phys. Chem. Minerals* **22** 524
[36] Cornell R M, Mann S and Skarnulis A J 1983 *J. Chem. Soc. Faraday Trans.* I **79** 2679
[37] Madsen M B, Mørup S and Koch C J W 1988 *Hyperfine Interact.* **42** 1059
[38] Wivel C and Mørup S 1981 *J. Phys. E: Sci. Instrum.* **14** 605
[39] Mørup S 1983 *J. Magn. Magn. Mater.* **37** 39
[40] Kuhn L T, Lefmann K, Bahl C R H, Ancona S N, Lindgård P-A, Frandsen C, Madsen D E and Mørup S 2006 *Phys. Rev.* B **74** 184406
[41] Brown W F 1963 *Phys. Rev.* **130** 1677
[42] Mørup S and Hansen B R 2005 *Phys. Rev.* B **72** 024418
[43] Jones D H and Srivastava K K P 1986 *Phys. Rev.* B **34** 7542
[44] van Lierop J and Ryan D H 2001 *Phys. Rev.* B **63** 064406
[45] Bødker F, Mørup S and Linderoth S 1994 *Phys. Rev. Lett.* **72** 282
[46] Bødker F and Mørup S 2000 *Europhys. Lett.* **52** 217
[47] Tronc E 1996 *Nuovo Cimento* D **18** 163
[48] Xu M, Bahl C R H, Frandsen C and Mørup S 2004 *J. Colloid Interface Sci.* **279** 132
[49] Koch C J W, Madsen M B, Mørup S, Christiansen G, Gerward L and Villadsen J 1986 *Clays Clay Miner.* **34** 17
[50] Madsen D E, Hansen M F, Koch C B and Mørup S 2008 *J. Phys.: Condens. Matter* **20** 135215
[51] Frandsen C *et al* 2008 unpublished